

Performance optimization of Si/Gd extreme ultraviolet multilayers

David L. Windt,^{1,*} Jeffrey A. Bellotti,¹ Benjawan Kjornrattanawanich,²
and John F. Seely³

¹Reflective X-ray Optics LLC, 1361 Amsterdam Ave, Suite 3B, New York, New York 10027, USA

²Universities Space Research Association, Brookhaven National Laboratory, Upton, New York 11973, USA

³Naval Research Laboratory, 4555 Overlook Avenue S.W., Washington, D.C. 20375, USA

*Corresponding author: davidwindt@gmail.com

Received 17 July 2009; revised 14 September 2009; accepted 15 September 2009;
posted 15 September 2009 (Doc. ID 114408); published 1 October 2009

We compare the performance, stability and microstructure of Si/Gd multilayers containing thin barrier layers of W, B₄C, or SiN_x, and determine that multilayers containing 0.6 nm thick W barrier layers at each interface provide the best compromise between high peak reflectance in the extreme ultraviolet near $\lambda = 60$ nm and good stability upon heating. The Si/W/Gd films have sharper interfaces and also show vastly superior thermal stability relative to Si/Gd multilayers without barrier layers. We find that these structures have relatively small compressive film stresses, and show good temporal stability thus far. We measured a peak reflectance of 29.7% at $\lambda = 62.5$ nm, and a spectral bandpass of $\Delta\lambda = 9$ nm (FWHM), for an optimized Si/W/Gd multilayer having a period $d = 32.0$ nm. © 2009 Optical Society of America
OCIS codes: 230.4170, 310.1620, 310.6860, 340.0340, 350.1260.

1. Introduction

Reflective multilayer films having nanometer-scale periods are now widely used for a variety of scientific and industrial applications in the extreme ultraviolet (EUV) region of the electromagnetic spectrum. For solar physics applications in particular, multilayer coatings operating near normal incidence in the EUV have enabled the construction of a number of spaceborne instruments over the past two decades of research, for both monochromatic imaging using telescopes coated with narrowband multilayers (e.g., [1]) and high-resolution spectroscopy using multilayer-coated gratings (e.g., [2]). There are several available multilayer material combinations, such as Mo/Y, Si/Mo, SiC/Si, and Si/Sc, that provide good optical performance in the EUV, and that have sufficiently high stability and low stress for use in solar instrumentation. But, while currently available mul-

tilayer coatings can be tuned to a number of different wavelengths in the approximate range $9 < \lambda < 50$ nm, corresponding to emission from particular spectral lines (or line complexes) that originate from ionized atoms in the solar atmosphere, all of the bright, well-isolated emission lines in this wavelength band arise from plasma formed at either low (e.g., He II, $\lambda = 30.4$ nm, $\log T = 4.7$) or high temperatures (Fe VIII, $\lambda = 13.1$ nm, $\log T = 5.9$; Fe IX, $\lambda = 17.1$ nm, $\log T = 6.0$; etc.) Thus, in practice, existing multilayer coatings are ill suited for observing well-isolated emission lines formed at intermediate temperatures in the solar atmosphere (i.e., in the approximate range of $4.7 < \log T < 5.9$), and so there remains an observational "gap," in that the solar plasma cannot yet be well sampled over a wide range of temperatures using currently available multilayers.

To fill the need for an efficient narrowband multilayer coating that can be used to observe an intermediate-temperature solar emission line, we have recently developed the Si/Gd multilayer system [3]

0003-6935/09/295502-07\$15.00/0
© 2009 Optical Society of America

for use near the O V line at $\lambda = 62.97$ nm, which is formed at $\log T = 5.4$ in the solar atmosphere. From detailed measurements of the Gd optical constants in the EUV, we discovered that this material has a narrow transmission “window” in the vicinity of the O V line, owing to unfilled $4f$ and $5d$ sublevels [4]. When used in combination with Si, the low absorption of Gd in the wavelength region near $\lambda = 63$ nm can be exploited to produce highly efficient, narrowband Si/Gd multilayers.

We have already reported on the initial development of the Si/Gd multilayer system [2]; that effort included a comparison of various materials (i.e., tungsten, boron carbide, and silicon nitride) that were tested for use as diffusion barriers at the Si–Gd interfaces to improve performance and stability. In this paper we describe a subsequent effort to systematically optimize the performance and stability of the Si/Gd system, using normal-incidence EUV reflectometry, grazing-incidence x-ray reflectometry (XRR), thermal annealing, transmission electron microscopy, and film stress measurements to guide the design of the thin barrier layers used at each interface so as to minimize diffusion. In the sections that follow, we describe our experimental techniques, present our results, and discuss their significance.

2. Experimental Procedures

The multilayer films discussed here were prepared by DC magnetron sputtering using a deposition system that has been described previously [5]. This system comprises three cathodes of two different types that each use solid, rectangular targets: the two larger cathodes used targets of Si (99.999% purity) and Gd (99.8% purity, excluding Ta), measuring $50\text{ cm} \times 9\text{ cm} \times 0.6\text{ cm}$, while the third, smaller cathode, needed only for samples containing W or B_4C barrier layers, used rectangular targets of either W (99.95% purity) or B_4C (99.5% purity), measuring $43\text{ cm} \times 7.4\text{ cm} \times 0.6\text{ cm}$. The cathodes were all operated in regulated power mode, with 600 W applied to the Si target, and 400 W applied to the Gd, W, or B_4C targets. The vacuum chamber is cryopumped, and the background pressure in the chamber prior to deposition was in the range of $1\text{--}3 \times 10^{-7}$ Torr in all cases. The sputter gas was Ar (99.999% purity), and the gas pressure was held constant at 1.60 ± 0.01 mTorr during deposition. For samples containing silicon nitride barrier layers, reactive sputtering of Si with an Ar/ N_2 gas mixture was used during barrier layer deposition. In that case, the sputter gas mixture was modulated during deposition, with pure Ar used for the Si and Gd layers, and an Ar/ N_2 gas mixture for the barrier layers. The Ar/ N_2 gas pressure was maintained at 1.6 mTorr during barrier layer deposition: the N_2 flow rate was 25 sccm and the Ar flow rate was 250 sccm, thus, the flowing gas contained 9.0% N_2 by volume. As the exact compositional stoichiometry of these nitride layers is unknown, we henceforth designate the reactively deposited material as SiN_x .

Multilayer films were deposited onto 75 mm diameter, prime-grade Si (100) wafers. Individual layer thicknesses were adjusted by varying the computer-controlled rotation rate, and hence the exposure time, of the substrate as it passes over each magnetron cathode. The effective deposition rates, computed using layer thicknesses determined from XRR measurements (described below) divided by the known exposure times, were found to be ~ 0.11 nm/s for Si, ~ 0.27 nm/s for Gd, ~ 0.052 nm/s for W, ~ 0.0017 nm/s for B_4C , and ~ 0.010 nm/s for SiN_x .

XRR measurements were made in the $\theta\text{--}2\theta$ geometry using a four-circle x-ray diffractometer having a sealed-tube Cu source and a Ge (111) crystal monochromator tuned to the Cu $K - \alpha$ line ($\lambda = 0.154$ nm, $E = 8.04$ keV). The angular resolution of this system is estimated to be $\delta\theta \sim 0.015^\circ$. Fits to the XRR data (performed using IMD software [6]) were used to determine the film thickness of single-layer films used for deposition rate calibrations, and to determine the period of multilayer films, with an estimated precision of $\delta d \sim \pm 0.01$ nm.

Transmission electron microscopy of selected samples was performed by Evans Analytical Group, Sunnyvale, California. Cross-sectional samples were prepared by the wedge polishing technique and then ion milled to electron transparency using 3 kV Ar^+ ions and a Gatan Model 691 Precision Ion Polishing System. Measurements were made using a JEOL model 2010 microscope operating at 200 keV.

Film stress was measured using a Toho Technologies Flexus model 2320S wafer curvature system. The curvature of the Si wafer substrates (0.4 mm nominal thickness) was measured along two orthogonal directions before and after film deposition. The total film thickness as determined by XRR was used to compute film stress, following the standard formalism based on the Stoney equation [7]. In addition, stress-versus-temperature measurements, from room-temperature (25 °C) to 300 °C, were made on selected multilayer samples using the same instrument.

The reflectance of selected samples was measured using synchrotron radiation at an incidence angle of 5° from normal, using the Naval Research Laboratory reflectometer on beamline X24C at the National Synchrotron Light Source (NSLS), Brookhaven National Laboratory. A dual-element monochromator utilizing a Au mirror and a 600 line/mm grating was used to generate a tunable, monochromatic pencil beam over the energy range $E = 11\text{--}465$ eV. The EUV reflectance was computed from the ratio of the reflected beam current to the incident beam current, both measured using the same Si photodiode after being normalized against the storage ring current decay.

3. Results and Discussion

During our previous, initial investigation [2], we compared the performance of Si/Gd multilayers with and without barrier layers of W, B_4C , or SiN_x , as a

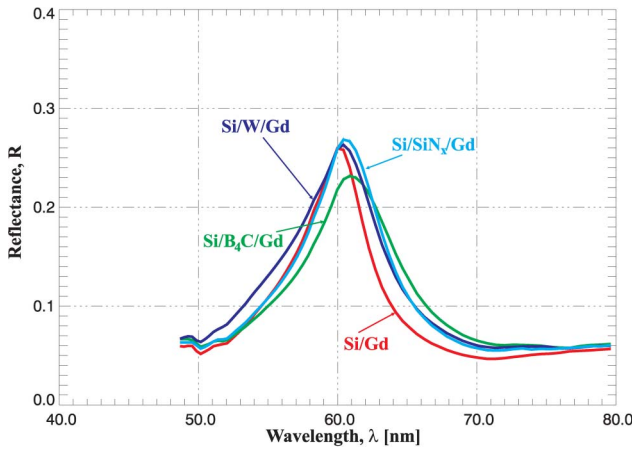


Fig. 1. (Color online) Measured normal-incidence reflectance of Si/Gd multilayers containing W, B₄C and SiN_x barrier layers as marked.

function of barrier layer thickness. (Identical barrier layers were deposited at both the Si-on-Gd and the Gd-on-Si interfaces.) Based on those results, a barrier layer thickness of 1 nm was selected for the thermal stability investigations that we discuss presently.

Shown in Fig. 1 are the measured reflectance-versus-wavelength curves for the four different (as-deposited) Si/Gd multilayers studied here, all having nominal 10.49 nm thick Si layers and 23.02 nm thick Gd layers, i.e., $\Gamma_{\text{Si}} = d_{\text{Si}} / (d_{\text{Si}} + d_{\text{Gd}}) \sim 0.3$; multilayers with barrier layers of W, B₄C, or SiN_x are shown in Fig. 1 along with the Si/Gd multilayer containing no barrier layers. The addition of either W or SiN_x barrier layers increases the peak reflectance by $\sim 1\%$, while the film having B₄C barrier layers has a peak reflectance that is $\sim 3\%$ lower than Si/Gd. All three multilayers containing barrier layers have a somewhat larger spectral bandpass than Si/Gd multilayers without barrier layers.

Shown in Fig. 2 are the measured reflectance data for three samples of each of these same four film designs after annealing, on a hot plate in air, for 1 h at 100 °C, 200 °C, and 300 °C, relative to the as-deposited films. Heating to 100 °C had no measurable effect on EUV reflectance in all four cases. At 200 °C, however, the Si/Gd, SiB₄C/Gd, and Si/SiN_x/Gd films all show shifts in peak wavelength; the Si/Gd and Si/B₄C/Gd films show significant decreases in peak reflectance, as well. On the other hand, the Si/W/Gd film is essentially unchanged after heating

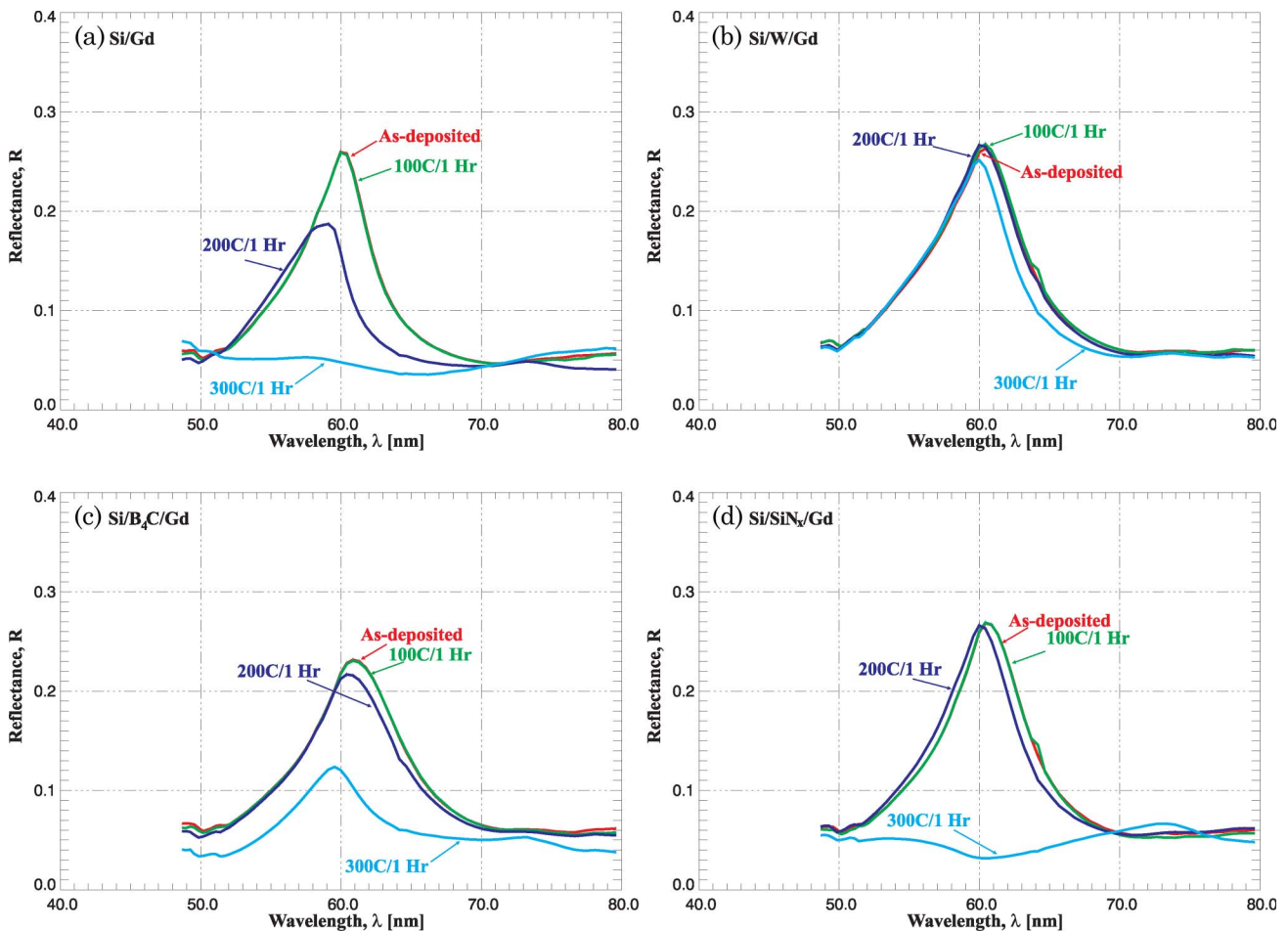


Fig. 2. (Color online) Measured normal-incidence reflectance for (a) Si/Gd, (b) Si/W/Gd, (c) Si/B₄C/Gd, and (d) Si/SiN_x/Gd multilayers that have been annealed for 1 h in air at 100 °C, 200 °C, and 300 °C, as marked.

to 200 °C. Upon heating to 300 °C, the Si/Gd and Si/SiN_x/Gd films show no Bragg peaks whatsoever, and the SiB₄C/Gd film peak height has decreased by more than a factor of 2. The Si/W/Gd film still shows relatively high reflectance after 300 °C annealing, with only a slight (~0.7 nm) shift toward shorter wavelengths. The changes in peak height and multilayer period apparent in the EUV data of Fig. 2 closely follow the peak height and period changes observed from XRR measurements, which we do not present here.

Based on the results of Fig. 2, we focused our attention on Si/W/Gd multilayers for the subsequent studies that are now described. Shown in Fig. 3 are high-resolution transmission electron microscopy (HRTEM) images of the as-deposited Si/Gd and Si/W/Gd multilayers shown in Figs. 1 and 2. The Si layers in these films are amorphous, while the Gd layers are polycrystalline, with a strong crystallite orientation in the direction of growth, as evidenced by the predominance of in-plane lattice fringes. Amorphous interlayers are clearly visible at both types of interfaces in the Si/Gd film; the apparent interlayer thickness is ~3.2 nm, as indicated. The apparent Si and Gd layer thicknesses in the Si/Gd film are ~9.2 and ~18.7 nm, respectively, and are substantially smaller than the nominal values listed above, presumably resulting, in part, from the formation of the amorphous interlayers just mentioned. Comparable interlayers are not evident in the Si/W/Gd film. However, the W barrier layers in this film have an apparent thickness of 1.8 nm, which is significantly larger than the 1.0 nm nominal value, suggesting that these layers may contain some Gd or Si in addition to W. In any case, the apparent Si and Gd layer thicknesses in the Si/W/Gd film are ~11.1 and ~21.0 nm, respectively, values much closer to nominal.

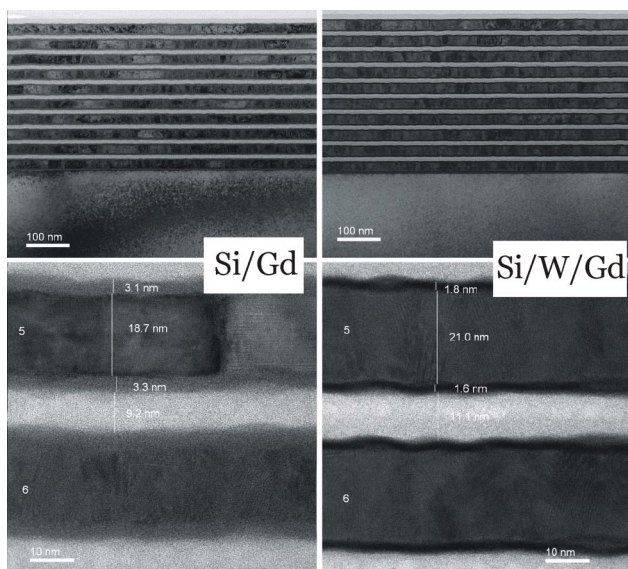


Fig. 3. (Color online) HRTEM images of as-deposited Si/Gd (left) and Si/W/Gd (right) multilayers.

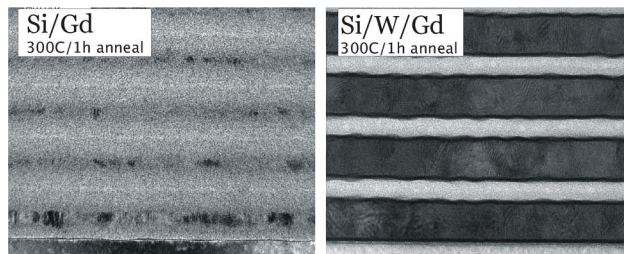


Fig. 4. (Color online) HRTEM images of Si/Gd (left) and Si/W/Gd (right) multilayers after annealing for 1 h at 300 °C.

Shown in Fig. 4 are HRTEM images of these same films after 300 °C annealing. While the layer structure is still evident after annealing in the Si/Gd film, the “pure” Si and Gd layers are much thinner, and the contrast between the Si and Gd layers is greatly reduced: the Si–Gd interlayers have apparently grown substantially, consuming most of the “pure” Si and Gd layers in the process. In contrast, the annealed Si/W/Gd film appears essentially unchanged, commensurate with the EUV results shown in Fig. 2 and discussed above. The thin W layers in this structure are evidently quite effective barriers against diffusion, at least up to 300 °C.

Shown in Fig. 5 are stress-versus-temperature results for Si/Gd and Si/W/Gd multilayer films identical to those just described in Figs. 3 and 4. For this experiment the samples were heated to 300 °C at a rate of 5°/min, then held at 300 °C for a period of 30 min, and finally allowed to cool to room temperature. As can be seen from Fig. 5, the stress in both films increases nearly linearly with temperature, up to about 90 °C, owing to the mismatch in thermal expansion coefficients between the film and substrate. Above 90 °C the film begins to relax, a change in stress that has been observed in many other Si-based multilayer systems, such as Si/Mo [8], and that has been attributed to viscous flow and possibly to density changes, as well. In any case, the stress decreases further in the Si/W/Gd film up to 300 °C, and then, upon cooling, the stress decreases nearly linearly, again due to the thermal expansion coefficient

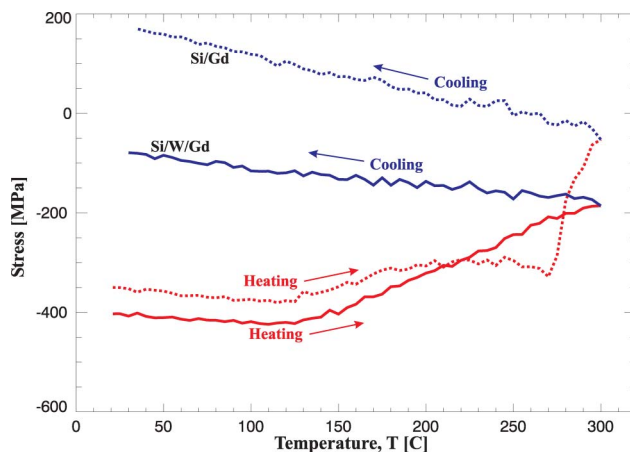


Fig. 5. (Color online) Film stress measured as a function of temperature for Si/Gd and Si/W/Gd multilayers.

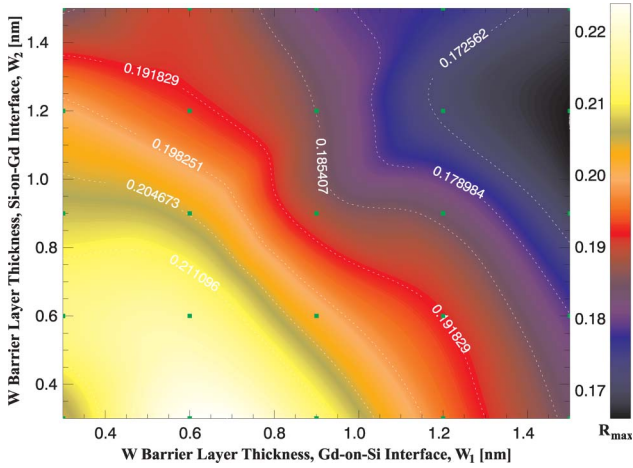


Fig. 6. (Color online) Measured peak reflectance as a function of the W barrier layer thickness at the Gd-on-Si and the Si-on-Gd interfaces, W_1 and W_2 , respectively. The small filled rectangles indicate the points at which measurements were made, while the smooth contours were computed using bilinear interpolation between these points.

mismatch. In contrast, the Si/Gd film without W barrier layers displays a more complicated behavior of stress with temperature above $\sim 200^\circ\text{C}$: unlike the Si/W/Gd film, above 200°C the stress in the Si/Gd multilayer remains approximately constant up to $\sim 270^\circ\text{C}$, and then the stress abruptly decreases by $\sim 175\text{ MPa}$ on further heating to 300°C ; upon cooling to room temperature, the stress again decreases linearly, as in the Si/W/Gd film. The large difference in stress–temperature behavior between the Si/Gd and Si/W/Gd films upon heating above 200°C is presumably associated with the growth of the Si–Gd interlayers suggested by the HRTEM images of Fig. 4; the EUV reflectance data of annealed Si/Gd films shown in Fig. 2—which suffer large performance change above 200°C —are also consistent with the hypothesized interlayer growth at these temperatures.

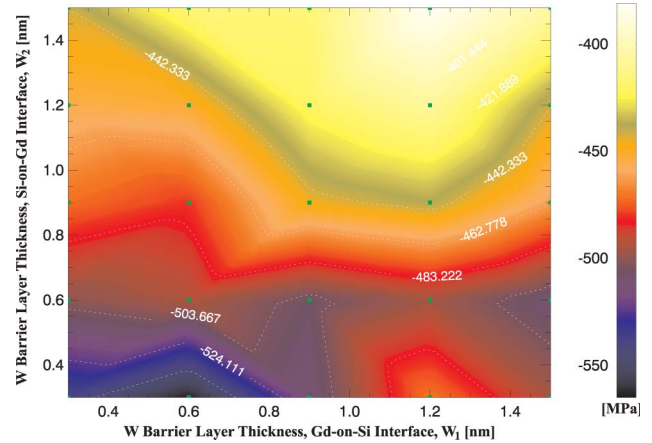


Fig. 7. (Color online) Measured film stress as a function of the W barrier layer thickness at the Gd-on-Si and the Si-on-Gd interfaces, W_1 and W_2 , respectively. The small filled rectangles indicate the points at which measurements were made, while the smooth contours were computed using bilinear interpolation between these points.

We next attempted to further optimize the performance of Si/W/Gd multilayers by systematically varying the W barrier layer thicknesses at each of the two types of interfaces independently. Specifically, we fabricated an array of 25 different Si/W/Gd multilayers, all having nominal Si and Gd layers of 10.49 and 23.02 nm thickness, respectively, in which the W layer thicknesses at the Gd-on-Si interface, denoted as W_1 , and at the Si-on-Gd interface, denoted as W_2 , were varied over the range of 0.3–1.5 nm, in increments of 0.3 nm. We measured both the normal-incidence reflectance and the film stress of each of the 25 resultant samples.

Shown in Figs. 6 and 7 are contour plots of peak reflectance and film stress, respectively, as a function of the two W barrier layer thicknesses, W_1 and W_2 . From Fig. 6 we see that the peak reflectance varies over the range of $16.5\% < R_{\text{max}} < 22.5\%$ for these samples, with a maximum in reflectance for $W_1 =$

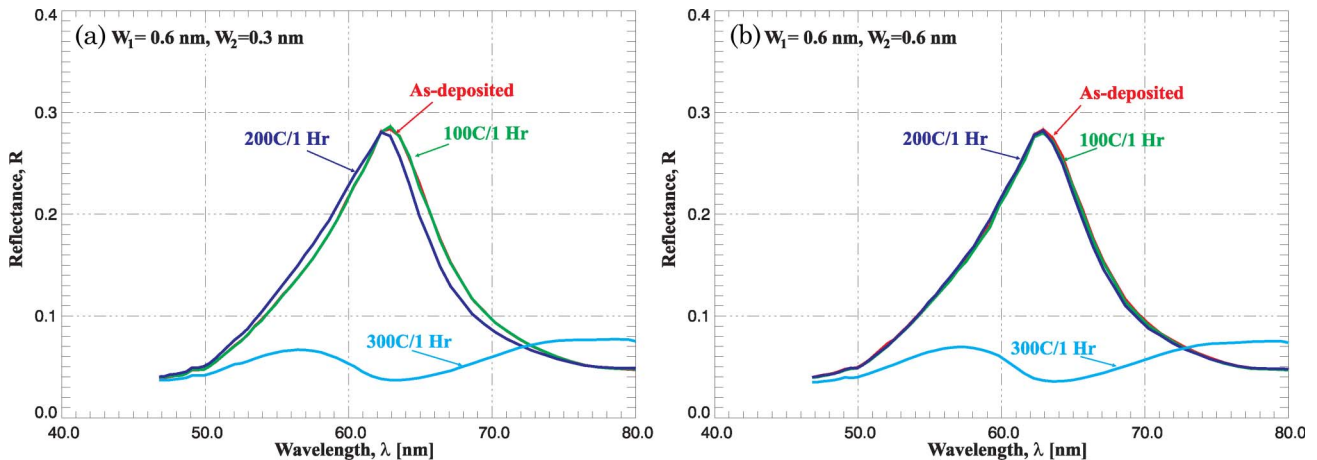


Fig. 8. (Color online) Measured normal-incidence reflectance for Si/W/Gd multilayers that have been annealed for 1 h in air at 100°C , 200°C , and 300°C , as marked. The films in (a) have barrier layer thickness $W_1 = 0.6\text{ nm}$ and $W_2 = 0.3\text{ nm}$, while the films in (b) have $W_1 = W_2 = 0.6\text{ nm}$.

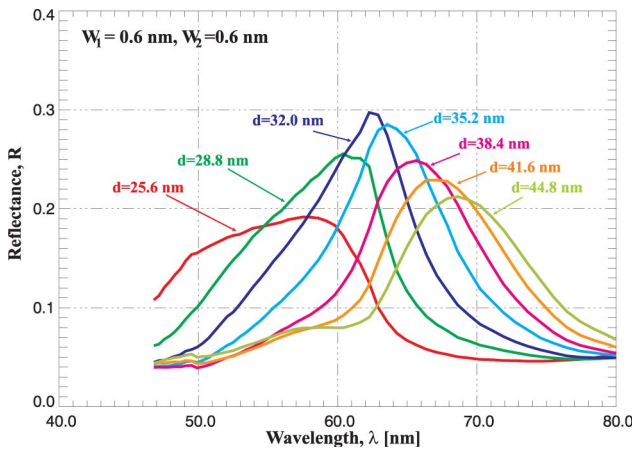


Fig. 9. (Color online) Reflectance versus wavelength of Si/W/Gd multilayers as a function of multilayer period d over the range $d = 25.6$ – 44.8 nm, as indicated.

0.6 nm and $W_2 = 0.3$ nm. Figure 7 reveals only a slow variation in film stress with W_1 and W_2 , with relatively small compressive stresses (less than -600 MPa) in all cases.

Based on the results shown in Figs. 6 and 7, we selected the two Si/W/Gd film designs having the highest peak reflectance for further thermal annealing studies: both films have $W_1 = 0.6$ nm, but one has $W_2 = 0.3$ nm and the other has $W_2 = 0.6$ nm. As for the films discussed above and shown in Fig. 2, for these two Si/W/Gd film designs, we performed 1 h thermal anneals on a hot plate in air, for three nominally identical samples of each of the two designs, at temperatures of 100 °C, 200 °C, and 300 °C, respectively. Each film was characterized after annealing (along with the as-deposited films) using XRR and normal-incidence EUV reflectometry. As is evident from the EUV results shown in Fig. 8, both films show no Bragg peak after heating to 300 °C, unlike the Si/W/Gd film with $W_1 = W_2 = 1.0$ nm shown in Fig. 2(b) that shows only a small change in reflectance after heating to 300 °C. However, while both

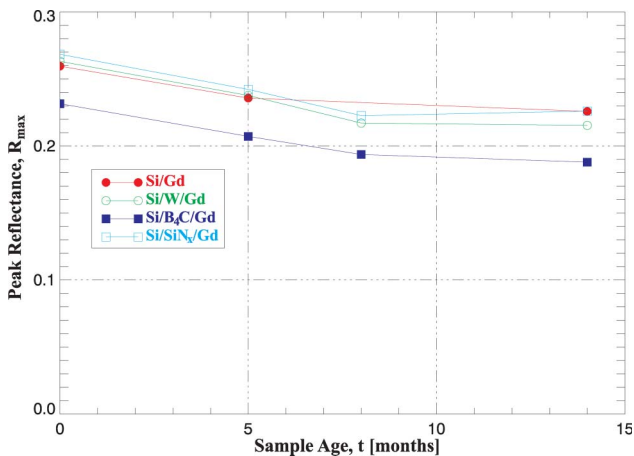


Fig. 10. (Color online) Peak reflectance measured periodically as a function of time for Si/Gd, Si/W/Gd, Si/B₄C/Gd, and Si/SiN_x/Gd multilayers as indicated.

films shown in Fig. 8 still have high reflectance after heating to 200 °C, the film having $W_2 = 0.3$ nm shows a significant wavelength shift (~ 0.8 nm, toward shorter wavelengths), whereas the film having $W_2 = 0.6$ nm is unchanged after heating to 200 °C. (Once again, peak height and period changes observed from XRR measurements obtained from these films are consistent with the EUV measurements shown in Fig. 8, but are not presented here.) In light of this last result, we have selected the design with $W_1 = W_2 = 0.6$ nm as the best compromise between high peak reflectance (for as-deposited films) and good thermal stability.

Having identified the optimal W barrier layer thicknesses as just described, we next fabricated a series of seven Si/W/Gd films with periods in the range $d = 25.6$ – 44.8 nm. All films have $W_1 = W_2 = 0.6$ nm, and all have a constant Si to Gd layer thickness ratio, namely $d_{\text{Si}}/(d_{\text{Si}} + d_{\text{Gd}}) = 0.3$. Shown in Fig. 9 are the normal-incidence reflectance data obtained from these seven films. It is obvious from Fig. 9 that the peak reflectance and spectral bandpass vary strongly with multilayer period, owing to the large variation in Gd optical constants over this range of wavelengths. The highest peak reflectance is found for the film having $d = 32.0$ nm, which gives $R_{\text{max}} = 29.7\%$ at $\lambda = 62.5$ nm, with a spectral bandpass of $\Delta\lambda = 9$ nm (FWHM). For larger or smaller multilayer periods, the peak reflectance is lower, and the spectral bandpass higher. In any case, the film having $d = 32.0$ nm is the most suitable of the series for monochromatic imaging or high-resolution spectroscopy of the O V line at $\lambda = 63$ nm near normal incidence.

Finally, to assess the temporal stability of Si/Gd multilayers, we show in Fig. 10 a plot of the peak reflectance as a function of time, measured periodically over a span of approximately 14 months, for the Si/Gd, Si/W/Gd, Si/B₄C/Gd, and Si/SiN_x/Gd multilayers shown in Fig. 1. All four films, which were stored in air at room temperature, show similar behavior: the peak reflectance steadily decreases by a few percent over the first ~ 8 months, and then remains essentially constant over time. No shift in peak wavelength was found (within experimental uncertainty). The initial reduction in reflectance shown in Fig. 10 is likely due to the growth of a thin a-SiO₂ surface layer at the topmost Si layer in these coatings. In any case, while we will continue to monitor the performance of these coatings over the coming years, our initial results as shown in Fig. 10 provide little evidence that these coatings will suffer from significant degradation over longer periods of time.

4. Summary and Conclusions

We have described our experimental efforts to characterize the performance, stability, and microstructure of Si/Gd multilayers containing thin barrier layers of W, B₄C, or SiN_x. We have determined that Si/W/Gd multilayers containing 0.6 nm thick W barrier layers at each interface provide the best

compromise between high peak reflectance in the EUV near $\lambda = 60$ nm and good stability upon heating. HRTEM indicates that these films contain amorphous Si layers and polycrystalline, oriented Gd layers. While Si/Gd multilayers without barrier layers show relatively large Si–Gd interlayers, films containing thin W barrier layers have significantly sharper interfaces and slightly higher peak reflectance. The Si/W/Gd films also show vastly superior thermal stability relative to Si/Gd multilayers without barrier layers. We find that these structures have relatively small compressive film stress (less than -600 MPa), and show good temporal stability thus far, with a drop in peak reflectance of a few percent occurring within the first eight months of storage in air, presumably due to the growth of a-SiO₂ at the top Si layer, and then no subsequent changes over time. We find an as-deposited peak reflectance of 29.7% at $\lambda = 62.5$ nm for an optimized Si/W/Gd multilayer having a period of $d = 32.0$ nm, and a spectral bandpass of $\Delta\lambda = 9$ nm (FWHM). Based on our investigations, we propose that Si/W/Gd multilayers can be used for high-resolution solar imaging and spectroscopy applications that target the O V line at $\lambda = 63$ nm ($\log T = 5.4$), which is presently the best candidate emission line for probing the solar atmosphere at intermediate temperatures in the EUV.

This research was sponsored by NASA Small Business Innovation Research contract numbers NNM07AA41C and NNM08AA24C.

References

1. J. P. Delaboudinière, G. E. Artzner, J. Brunaud, A. H. Gabriel, J. F. Hochdez, F. Millier, X. Y. Song, B. Au, K. P. Dere, R. A. Howard, R. Kreplin, D. J. Michels, J. D. Moses, J. M. Defise, C. Jamar, P. Rochus, J. P. Chauvineau, J. P. Marioge, R. C. Catura, J. R. Lemen, L. Shing, R. A. Stern, J. B. Gurman, W. M. Neupert, A. Maucherat, F. Clette, P. Cugnon, and E. L. Van Dessel, "EIT: extreme-ultraviolet imaging telescope for the SoHO mission," *Sol. Phys.* **162**, 291–312 (1995).
2. J. F. Seely, C. M. Brown, D. L. Windt, S. Donguy, and B. Kjørnattanawanich, "Normal-incidence efficiencies of multilayer-coated laminar gratings for the extreme-ultraviolet imaging spectrometer on the Solar-B mission," *Appl. Opt.* **43**, 1463–1471 (2004).
3. B. Kjørnattanawanich, D. L. Windt, and J. F. Seely, "Normal-incidence silicon–gadolinium multilayers for imaging at 63 nm wavelength," *Opt. Lett.* **33**, 965–967 (2008).
4. B. Kjørnattanawanich, D. L. Windt, J. A. Bellotti, and J. F. Seely, "Measurement of dysprosium optical constants in the 2–830 eV spectral range using a transmittance method, and compilation of the revised optical constants of lanthanum, terbium, neodymium, and gadolinium," *Appl. Opt.* **48**, 3084–3093 (2009).
5. D. L. Windt and W. K. Waskiewicz, "Multilayer facilities required for extreme-ultraviolet lithography," *J. Vac. Sci. Technol. B* **12**, 3826–3832 (1994).
6. D. L. Windt, "IMD—software for modeling the optical properties of multilayer films," *Comput. Phys.* **12**, 360–370 (1998).
7. G. G. Stoney, "The tension of metallic films deposited by electrolysis," *Proc. R. Soc. A* **82**, 172–175 (1909).
8. R. R. Kola, D. L. Windt, W. K. Waskiewicz, B. E. Weir, R. Hull, G. K. Celler, and C. A. Volkert, "Stress relaxation in Mo/Si X-ray multilayer structures," *Appl. Phys. Lett.* **60**, 3120–3122 (1992).